



Computational Analysis and Design Improvement of an Industrial Centrifugal Pump with Experimental Validation

Dhruva Patil¹ · Dhruv Bhandari¹ · Anjaneya Gorkal¹ · J. R. Nataraj¹

Received: 11 June 2019 / Accepted: 3 February 2020 / Published online: 14 February 2020
© The Institution of Engineers (India) 2020

Abstract Centrifugal pumps are one of the work horses in any process industries. Over the past few years, efforts to increase the performance of the centrifugal pump by various means have been ongoing. The performance of centrifugal pump is significantly affected by the path the fluid traverses along the geometry of blade and casing of the pump. Visualization of the fluid flow is difficult to comprehend. In the present work, commercial computational fluid dynamics (CFD) code, ANSYS CFX package is used to numerically simulate the 3D flow of water inside an industrial centrifugal pump. The effect of changing the volute geometry at regions of interest is studied. Steady-state analysis is performed using shear stress transport (SST) turbulence model using mixing plane interface between moving and stationary zones of the pump. Further, transient simulation using sliding mesh interface was carried out using results obtained from steady analysis as initial conditions. From the above results, recirculation was observed in the casing and minor losses near the neck region of the pump. Based on the results of transient simulation, the casing area was reduced at 2 regions by 4%, 8% and 12% to understand its effect on recirculation and minor losses. The results of transient analysis on the casing geometry showed that 8% reduction in area improved the pump efficiency by 4.85% at the design flow rate of 111.11 kg/s. The efficiency improvement of the pump is attributed to the reduction in recirculation and minor losses. The improvements in the efficiency were validated by

experimental results. The experimental results showed an improvement of efficiency by 4.62%.

Keywords Centrifugal pump · Computational fluid dynamics · Recirculation losses · Validation · SST

Introduction

Centrifugal pumps are undisputed machines of choice, especially for delivering liquid from one location to another by centrifugal action in numerous industries including agriculture, municipal (*water and wastewater plants*), process industries, power generation plants, petroleum and many other industries. The conventional approach of designing casing and impeller of pump was primarily theoretical with significant approximations. The pump from the theoretical model would then be manufactured as per the dimensions. The efficiency and performance curves of the manufactured pump were experimentally determined. This process is rather tedious, cumbersome and expensive in practice, and designed efficiency is usually not achieved. Theoretical models only give performance characteristics of pump, but they are not able to identify the areas of flow separation or recirculation with reliable accuracy [1]. Computational fluid dynamics (CFD) tools such as CFX are prevalent since more than 30 years [2–4] and are capable enough to precisely visualize the flow pattern of fluids in the pump. The computing power has grown exponentially over the past few decades. Along with it, the complexity of the CFD models has grown as well. This has resulted in wide usage of CFD to understand complex flows and study various designs of flow passages. The insights gained from CFD simulations

✉ Dhruva Patil
dhruvapatil98@gmail.com

¹ Department of Mechanical Engineering, RV College of Engineering, Bengaluru, India

are being used to improve the performance of pumps [5]. CFD analysis of pump requires adequate boundary conditions and defining of interfaces between rotating and stationary frames. The three main types of interfaces available in CFD codes are frozen rotor, mixing plane and sliding mesh interface. The first two interfaces are used to analyze steady-state approaches while the last one is used for transient simulations. In mixing plane method, flow data through the interface are circumferentially averaged and steady analysis performed in each fluid region. White et al. [6] experimentally validated this method and showed close match of the experimental results with simulation values. However, the accuracy of steady analysis is limited for it is inherently approximate.

There are few studies on the effect of changing the volute dimensions, primarily performed using steady analysis. Kim et al. [7] analyzed centrifugal pump performance by optimizing the impeller and volute profile to improve the performance. They observed that varying the cross-sectional area of the volute greatly affects the efficiency and head generated by the pump. A volute with 90% of their initial cross-sectional area was found to give the best results in their studies. A study on the effect of volute geometry observed that increasing the volute cross-sectional area reduced the efficiency and head at best efficiency point [8]. There are many more studies done in implementing CFD for optimizing centrifugal pumps and other turbomachinery, including researches on impeller modification [9–16].

Due to the success and advantages of using CFD in academic applications, more industries are incorporating simulations into their design methodology. This article discusses one such application where CFD simulations were used to improve the efficiency of an industrial centrifugal pump.

A 3D steady and transient analysis was performed on the centrifugal pump, including its volute. The procedure for the analysis, including fluid domain generation, meshing, brief description of the setup of steady and transient analysis, is mentioned. The numerical results are compared with experimental results, and sufficient correlation is found between the two.

Geometry and Meshing of Centrifugal Pump

The specifications of the pump considered for the study are given in Table 1. A 3D model based on CAD drawings was modeled in Unigraphics software and is shown in Fig. 1. The model was then converted into the necessary CFD model containing only the fluid region. This consists of three main domains and is shown in Fig. 2: the inlet region (Fig. 2a) which is cylindrical in shape; the impeller region

Table 1 Pump specifications

Parameter	Value
Design flow rate	111.11 kg/s
Angular velocity	1440 rpm
Operating inlet pressure	1 atm
Fluid	Water
Blade type	Backward twisted blades
Impeller diameter	298 mm
Impeller thickness	50 mm

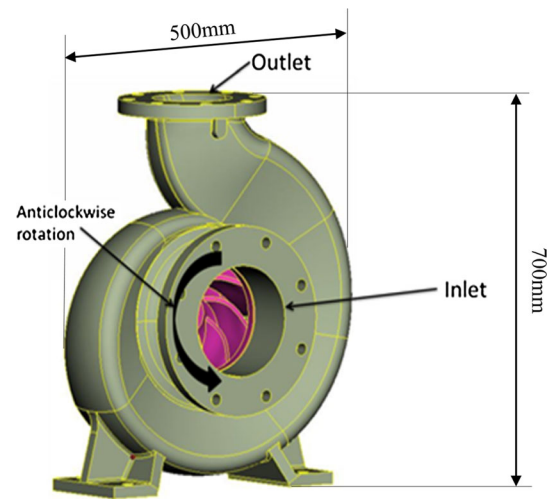


Fig. 1 CAD model of centrifugal pump

(Fig. 2b); and the casing region (Fig. 2c). The impeller blades and the shroud were carved out of first two domains to give only the fluid region where the water flows.

Meshing

The mesh model was generated using ANSYS software. The parameters used to generate the mesh are shown in Table 2. The resulting mesh has a y-plus value of 50. Due to the complexity of the profile, tetrahedral elements were used. The number of elements in the casing, impeller zone and the inlet was 3,969,093, 2,942,774 and 39,110, respectively, which adds up to 6,950,977 global elements. Figure 3 shows the mesh generated with the boundary layers for each region.

ANSYS CFX Setup and Boundary Conditions

The initial boundary conditions required for the simulation are defined as per Table 3. The rotating–stationary interface is modeled using mixing plane in the steady analysis and transient-rotor stator in the transient analysis. The

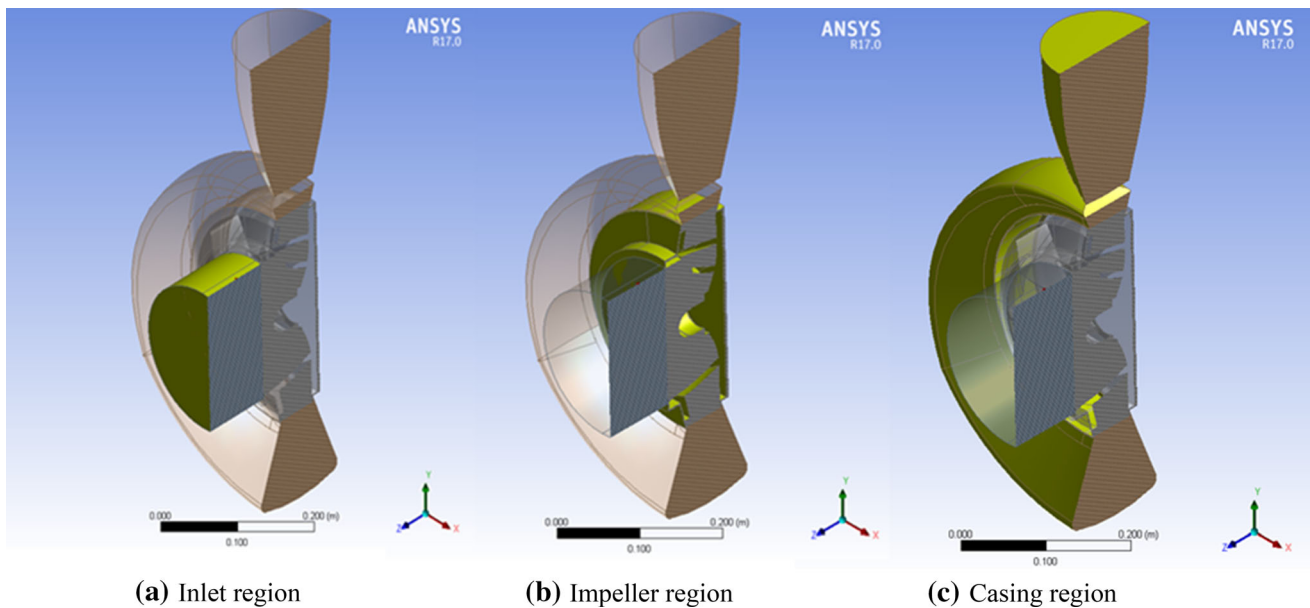


Fig. 2 Three regions created for CFD analysis

Table 2 Mesh generation

Property	Value	
Global size	5 mm	
Method	Adaptive for casing and inlet, patch conforming for impeller zone	
Inflation/boundary layer	First layer thickness	0.1 mm
	Number of layers	9
	Growth rate	1.3
Face sizing	Casing	3 mm
	Impeller	2 mm

steady-state results are taken as initial conditions for the transient analysis.

Steady-state analysis was not sufficient to fully capture the flow of fluid inside the pump due to the inherent transient nature of the problem, and hence, the values obtained for the flow variables by steady-state flow are not completely indicative of real-world behavior. However, they serve as good starting point for transient simulations.

Steady-state analysis was run until the RMS (root-mean-square) of residuals reached 2×10^{-4} . The results obtained were fed to transient analysis as its initial condition. The time step was set to 0.0003 s. Each time step ran multiple inner loops until the RMS of residuals converged to 1×10^{-4} . A total of 150 total time steps were run, which is equal to 0.045 s of real time. The results obtained in the transient simulation were averaged over last 50 time steps. The impeller rotates 1.08 cycles in 0.045 s. Since the blades are symmetric, to check for periodic steady state, it needs to rotate a multiple of $(1/n)$ cycles, where n is the

number of blades ($n = 8$). When the pump rotates 1/8th of a cycle, the blades move to the position where the adjacent blade was when the cycle began. Therefore, 1.08 cycles correspond to about 8 full time periods for the system. Further, the residuals also showed a consistent behavior over the simulation as seen in Fig. 5.

All the simulations were carried out on an Intel i7 3rd Gen (3.7 Ghz) processor and 12-GB RAM. Each steady analysis took about 8 h to complete, and transient analysis took about 15 h to complete.

The total head was calculated by considering the mass average of total pressure at inlet and at outlet, and the total head is calculated using Eq. (1).

$$H = \frac{P_{o2} - P_{o1}}{\rho g} \tag{1}$$

Torque was calculated using CFX’s inbuilt calculator on the blade’s surfaces. Using the torque, input power was found by multiplying torque with angular velocity of the impeller blades as shown in Eq. (2).

$$P_{input} = \tau * \frac{2\pi N}{60} \tag{2}$$

The above two values are used to calculate hydraulic efficiency of the pump using Eq. (3).

$$\eta = \frac{\dot{M}gH}{P_{input}} \tag{3}$$

Governing Equations and Choosing Turbulence Models

Turbulence is a physical phenomenon characterized by random and chaotic three-dimensional vorticity of fluid and

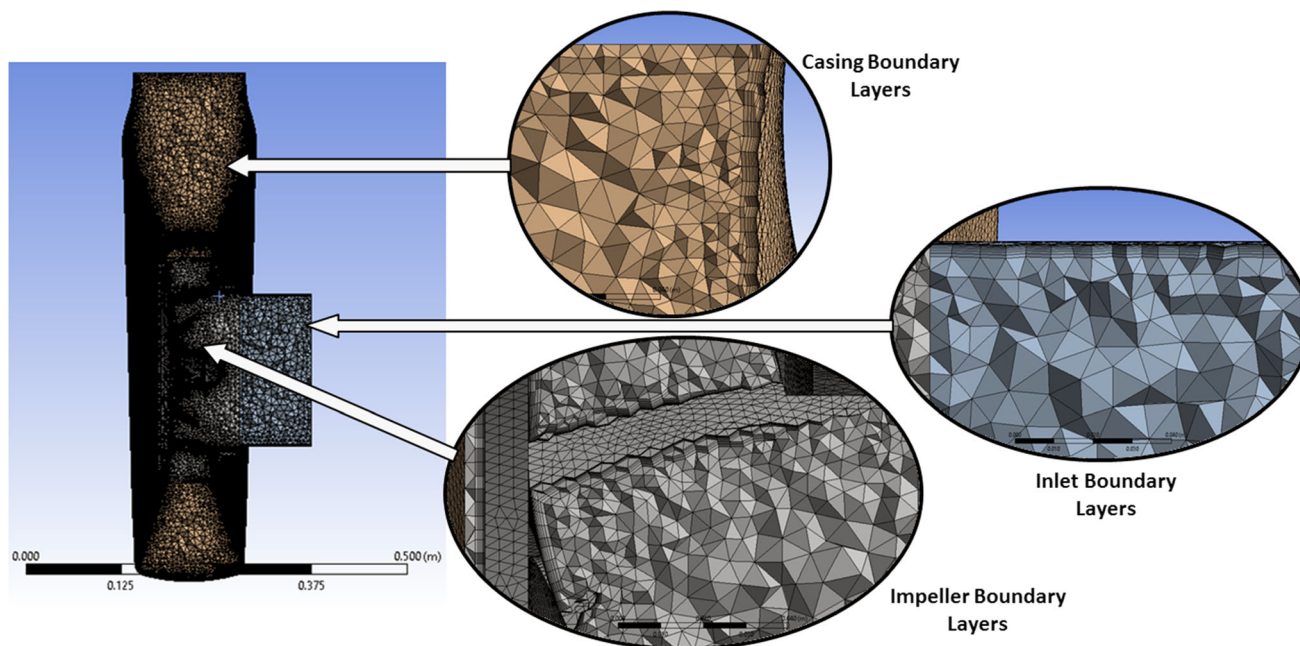


Fig. 3 Generated mesh

Table 3 Boundary conditions

Parameter	Value/condition
The static inlet pressure	1 bar absolute
Impeller zone	Modeled as rotating region with an angular velocity of 1440 rpm in counterclockwise direction
Water density	998 kg/m ³
Volute and inlet pipe	Modeled as stationary
Outlet mass flow rate	111.11 kg/s (400 m ³ /h)
Condition for walls	No-slip and smooth

chaotic changes in pressure. The presence of turbulence dominates over all other flow phenomenon, increasing energy dissipation, mixing, drag and heat transfer. Therefore, it is of great importance to model the turbulence phenomenon accurately.

The turbulence model, shear stress transport (SST), is a popular model to simulate most phenomenon as it captures the flow regime close to the wall as well as far away from it with the most accuracy [17, 18]. The SST model uses a mixing function value to automatically switch between $k-\omega$ (k -omega) and $k-\epsilon$ (k -epsilon) when close to or far away from a wall, respectively. The use of $k-\omega$ near the wall, where there would be boundary layer formation, makes the model directly usable all the way down to the wall, including the viscous sublayer. Hence, the SST model can

be used as a low-Reynolds turbulence model as well. Switching to $k-\epsilon$ away from the wall avoids the common problem associated with $k-\omega$, that is, the high sensitivity of the model in free-stream regions to inlet free-stream turbulence properties.

This model modifies the energy prediction term in the kinetic energy transfer equation.

Equations (4) and (5) model the turbulence of flow according to SST theory and are used in CFX:

- Equation (4) gives us the kinetic energy transfer (k) in the fluid

$$\frac{\partial(\rho k)}{\partial t} + \frac{\partial(\rho u_j k)}{\partial x_j} = P - \beta^* \rho \omega k + \frac{\partial}{\partial x_j} \left[(\mu + \sigma_k \mu_t) \frac{\partial k}{\partial x_j} \right] \tag{4}$$

- Equation (5) gives us the specific rate of dissipation (ω) and how it is transferred in the fluid

$$\frac{\partial(\rho \omega)}{\partial t} + \frac{\partial(\rho u_j \omega)}{\partial x_j} = \frac{\gamma}{v_t} P - \beta \rho \omega^2 + \frac{\partial}{\partial x_j} \left[(\mu + \sigma_\omega \mu_t) \frac{\partial \omega}{\partial x_j} \right] + 2(1 - F_1) \frac{\rho \sigma_\omega}{\omega} \frac{\partial k}{\partial x_j} \frac{\partial \omega}{\partial x_j} \tag{5}$$

Here, P is the pressure, ρ is the density of fluid, μ is the viscosities in fluid, u is the velocity of fluid, and F_1 is the mixing factor that determines whether $k-\omega$ is used or $k-\epsilon$.

Results and Discussion

The simulation of the existing pump gave results very close to the experimental values and theoretically calculated values. The CFD simulations gave a head of 19.383 m, while the experimental value is 19.935 m. The steady and transient analysis residuals are shown in Figs. 4 and 5. The transient residuals show a lot of variation as the residuals drop to 1×10^{-4} for each time step after at least five inner iterations. When the computation begins for the next time step, the residuals increases to almost 1×10^{-3} and the inner iterations start again. However, the residuals at the end of each time step did not vary significantly over the run, indicating a converged solution.

Mesh Independence Test

The mesh independence test was performed with three different mesh sizes. The results are shown in Table 4. The number of elements of each of the trials was 5.49 million, 6.87 million and 8.24 million, respectively. The total head, pressure head, torque, power and efficiency were considered as variables to study mesh convergence test. It is seen that the quantities vary considerably when comparing the 1st mesh with the 2nd (total head varies by 10% and pressure head by 12%). However, there is no significant variation between the 2nd and 3rd meshes (total head varies by 1% and pressure head by 0.6%). Hence, the mesh with 6.9 million elements was considered for the study, as that was significantly faster to compute.

Existing Pump CFD Analysis

The results of steady and transient simulation are tabulated in Table 5. The values obtained by mixing plane (steady)

for the total head and pressure head are lower by about 3% and 7%, respectively, when compared to transient results. However, the torque predicted in steady analysis is lower as well, leading to almost identical efficiency.

There are two regions observed in existing pump showing flow separation and minor losses as shown in Figs. 6 and 7. The losses observed are discussed below.

Figure 7 shows the transient results at the two regions of interest for existing pump. The first region (Fig. 7a) shows the left side of the casing, and recirculation is observed. Recirculation occurs when two layers of fluid have different velocity, causing a net torque at the interface due to friction. One of the reasons for recirculation is that the fluid reaching the region with the vortex from the top of the casing has a higher velocity compared to fluid leaving the impeller at that region. The fluid leaving the impeller is encountering a greater volume than the flow conditions require. This causes its velocity to decrease and results in recirculation once it encounters fluid from above. This can be corrected by reducing the area at this region causing the fluid leaving the impeller to attain sufficiently high velocity to match the fluid from above. However, reducing too much area could lead to the same phenomenon, in the opposite direction

The second region (Fig. 7b) shows the neck of the casing where the velocity magnitude is seen to drop. The fluid is encountering more volume than it needs, to flow through it, at that flow rate. This would result in minor loss due to sudden expansion at the neck. This problem can also be addressed by reducing the area.

Steady State Versus Transient Results

In this section, results of steady-state and transient analysis of the original pump are discussed. The results of steady

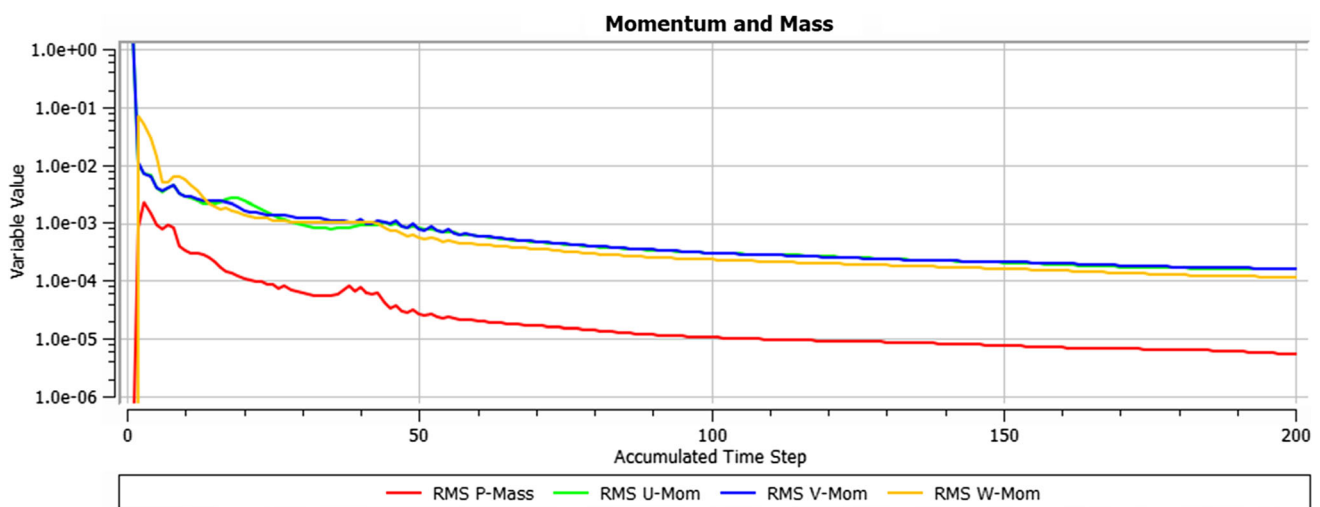


Fig. 4 Steady analysis residuals

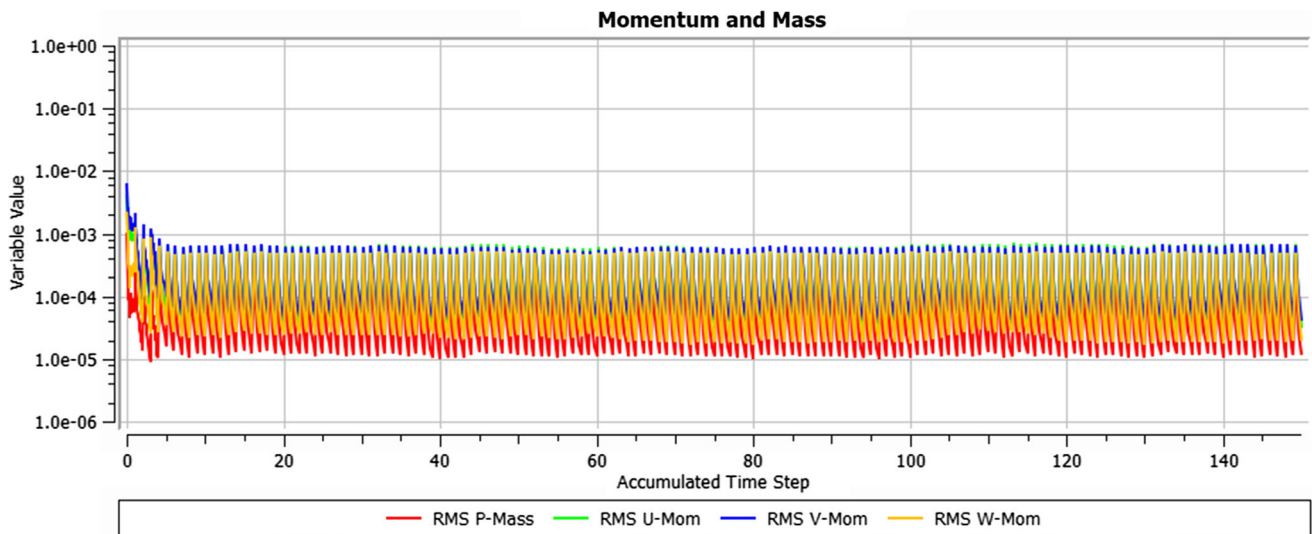


Fig. 5 Transient analysis residuals

Table 4 Mesh independence study

Mass flow rate (kg/s)	Number of elements	Total head (m of water)	Pressure head (m of water)	Torque (Nm)	Power (kW)	Efficiency (%)
111.11	5,488,612	16.93	15.32	178.98	26.99	68.38
	6,875,383	18.74	17.16	186.18	28.08	72.74
	8,237,510	18.54	17.05	186.01	28.05	72.03

Table 5 Steady and transient analysis results

Mass flow rate (kg/s)	Analysis	Total head (m of water)	Pressure head (m of water)	Torque (Nm)	Power (kW)	Efficiency (%)
111.111	Steady	18.736	17.165	186.179	28.075	72.742
	Transient	19.383	18.468	192.560	29.037	72.806

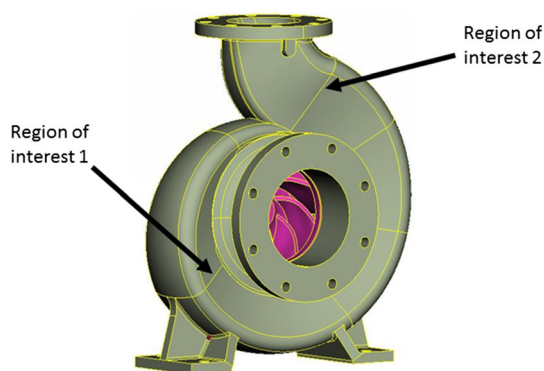


Fig. 6 Region of interest 1 and region of interest 2 of the pump and transient simulations are shown in Table 5. It is seen that the mixing plane analysis underestimates the pressure head compared to the sliding mesh (transient analysis) and underpredicts the total head as well.

The difference in predictions can be attributed to the nature of mixing plane analysis. Here, the pressure and velocity quantities from the impeller are averaged over the interface between rotor and stator and fed into the casing resulting in inaccuracies. The effects of fluid flow in the casing are not referred back to the impeller accurately in steady state. In reality, the backflow from the casing interacts with the fluid in the impeller in an unsteady manner due to the inertia of the fluid. This is completely lost in steady-state analysis. Similar behavior was observed by Voorde et al. [19] in their studies. Due to this, we get erroneous results. However, the overall flow passages obtained are sufficient to serve as a good initial condition for transient analysis, which would help to converge the transient simulation in fewer cycles.

Figures 8 and 9 show the first region of interest from steady and transient analysis, respectively. Figure 8

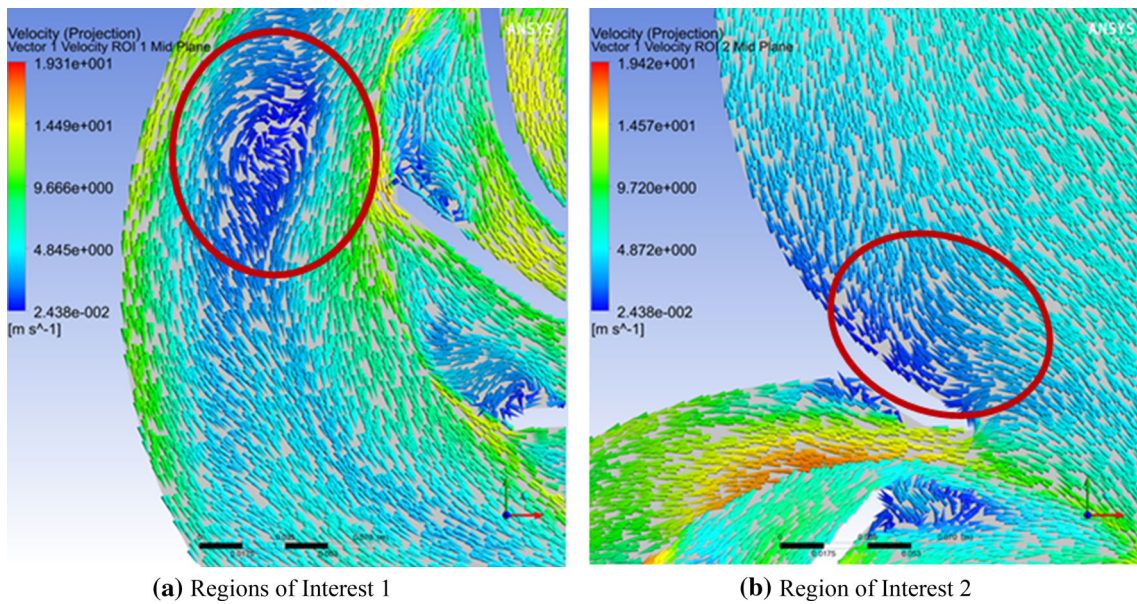


Fig. 7 Velocity vectors at regions of interest—transient results

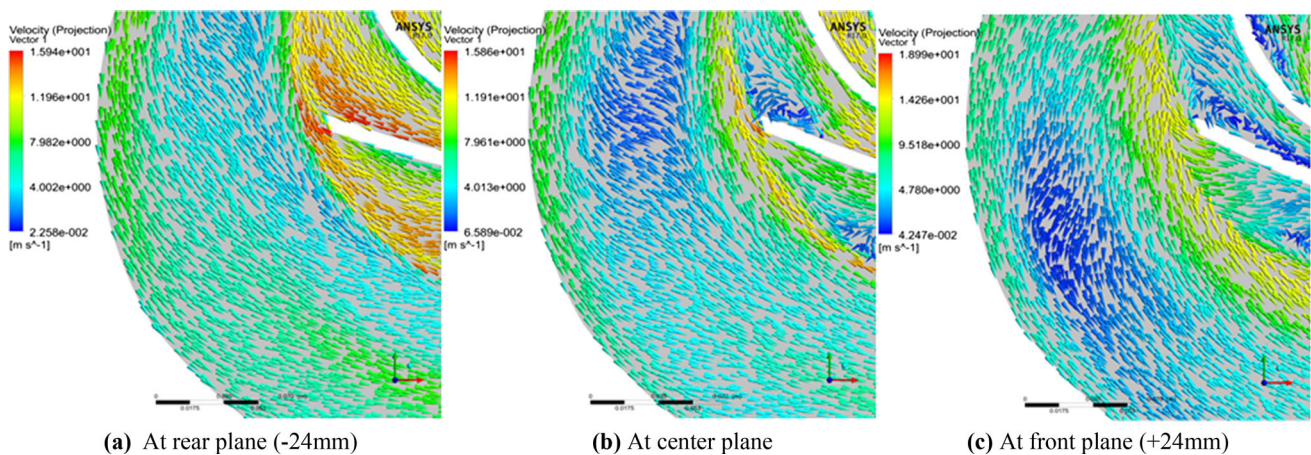


Fig. 8 Steady-state results of velocity vectors at left side of casing

indicates regions where the flow velocity drops and is significant in the front plane. The drop in velocity cannot be easily explained using steady analysis. From the steady analysis images, one could argue that the reason for the drop is due to water expanding and slowing down to occupy extra volume. However, fluid generally mixes chaotically when free volume is encountered inside an enclosure; instead, the steady data make it look like the fluid mostly maintains its streamline and only slows down. The transient image gives a more realistic explanation. As explained above, the extra volume allows for fluid from impeller to expand and slow down relative to layers above it, causing a mismatch in velocity and leading to vortices. This results in loss of energy of the fluid, leading to lower

efficiency. The solution in this case as well is to modify the design by reducing the area so as to ensure less vortices.

Figures 10 and 11 show the second region of interest for steady and transient analysis, respectively. The steady results show an isolated region of low flow velocity above the neck. Considering flow direction, this is not very realistic. The sudden transition near the neck should be causing a greater drop in velocity than a place significantly upstream of the obstruction. Transient results show a more realistic scenario of flow getting obstructed and losing velocity close to the transition region.

Even though steady and transient analysis led us to similar conclusions of design change, the transient analysis is still important to gain a better understanding of the real

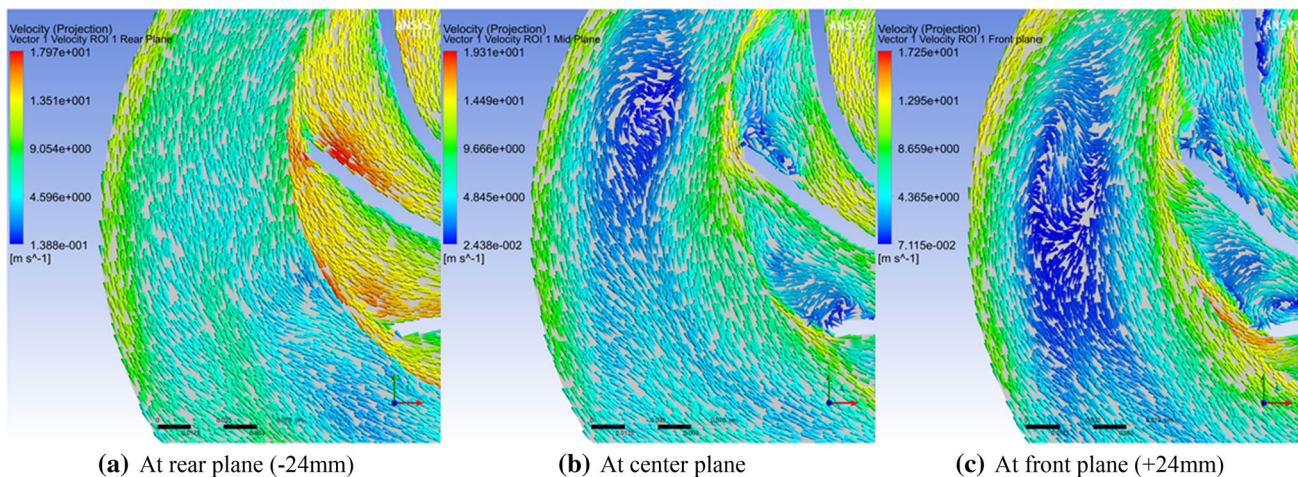


Fig. 9 Transient results of velocity vectors at left side of casing

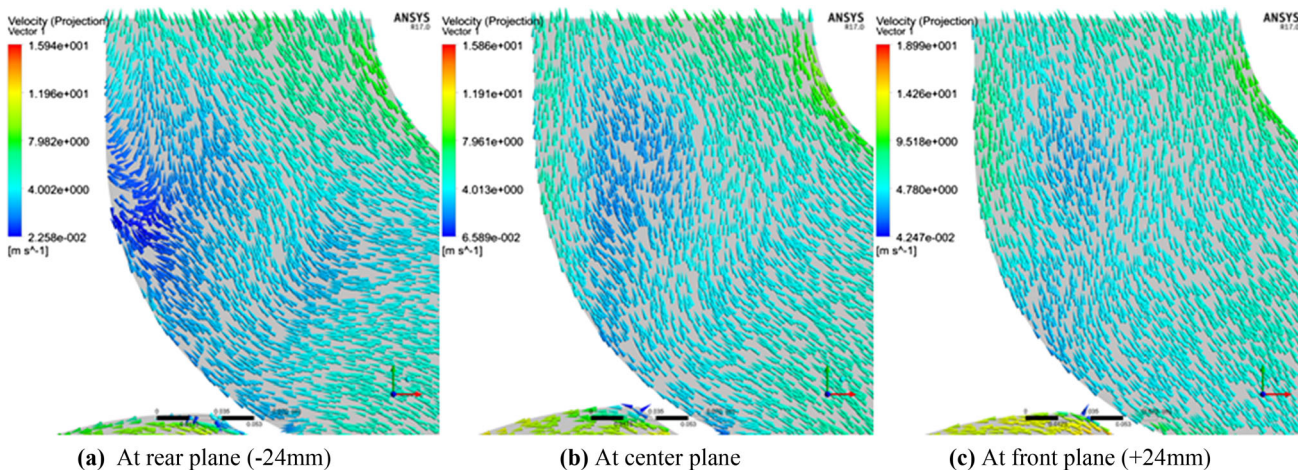


Fig. 10 Steady analysis results of velocity vectors at the neck region

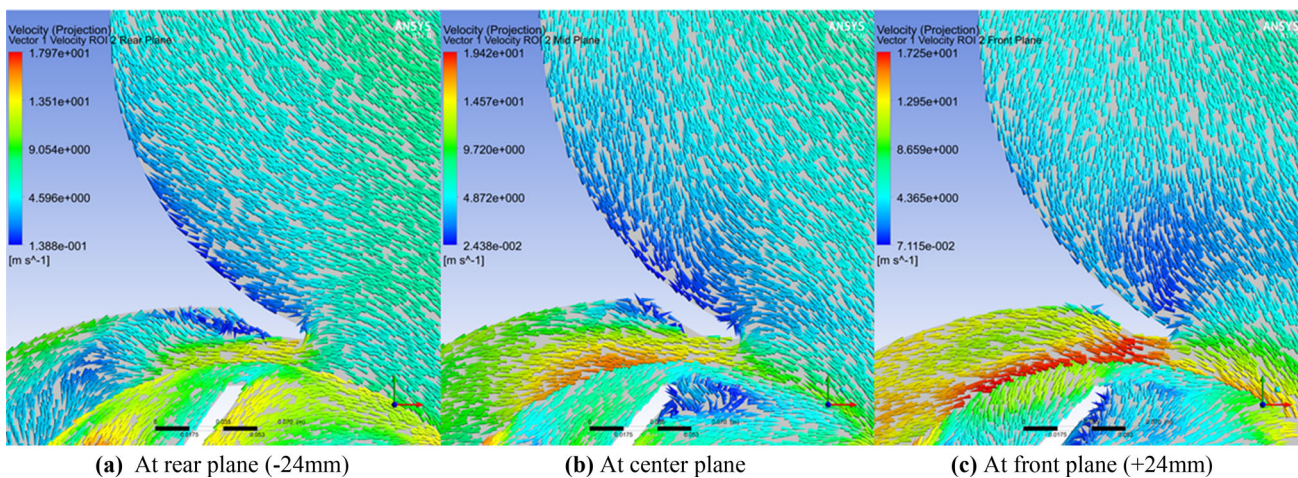


Fig. 11 Transient analysis results of velocity vectors at the neck region

cause of the loss and to detect regions of recirculation that would otherwise be missed.

Effects of Change in Casing Dimensions (Reduction in Area of the Casing)

The centrifugal pump was modified at two regions as shown in Fig. 6. The cross-sectional area in the existing pump is $6.5 \times 10^{-3} \text{ m}^2$ and $1.88 \times 10^{-2} \text{ m}^2$ at region of interest 1 and region of interest 2, respectively. The cross-sectional area at those regions was reduced by 4%, 8% and 12%, respectively. The transient results of the existing and modified casings are summarized in Table 6. The modified pump having 8% reduction in area at the two regions was found to give the highest efficiency compared with 4% and 12% area reduction. The results of model having highest efficiency (8% reduction in area) were chosen for further comparison with the existing pump model.

Figures 12 and 13 show velocity vectors at the first region of interest. Figure 12 shows regions of recirculation at various cut planes in the existing centrifugal pump. Figure 13 shows the same region with a smaller cross section (8% less). No recirculation is observed in this region. The velocity obtained by fluid leaving the impeller

is sufficient enough to not cause vortices when it encounters fluid from above. Figure 12b, c shows maximum recirculation regions in the existing pump, whereas it has completely disappeared in the modified pump (Fig. 13b, c).

Figures 14 and 15 show velocity vectors in the second region of interest. In Fig. 14, a drop in velocity magnitude is observed. In the modified pump (Fig. 15), the flow is more streamlined, with no significant drop in velocity as in existing pump. The modified pump in Fig. 15c shows a considerable improvement in the uniformity of velocity vectors when compared to Fig. 14c (existing pump) in the front plane.

These two effects combined caused the efficiency to increase from 72.806 to 76.345% at design flow rate, a 4.85% improvement.

Comparison of 4%, 8% and 12% Area Reduced Models

The CFD results of 4%, 8% and 12% area reduced models are compared here for a mass flow rate of 111.111 kg/s. Figures 16 and 17 show transient results for 4%, 8% and 12% reduced area models at region of interest 1 and region of interest 2, respectively. 8% area reduced model shows a clear improvement in terms of uniformity of flow and flow

Table 6 Existing and modified casing results

Mass flow rate (kg/s)	Pump	Total head (m of water)	Pressure head (m of water)	Torque (Nm)	Power (kW)	Efficiency (%)	% Increase in efficiency
111.111	Existing	19.383	18.468	192.560	29.037	72.806	–
	4% reduced	20.958	16.781	201.729	30.420	75.129	3.18
	8% reduced	21.092	17.542	199.776	30.126	76.345	4.85
	12% reduced	20.544	16.695	202.856	30.589	73.216	0.56

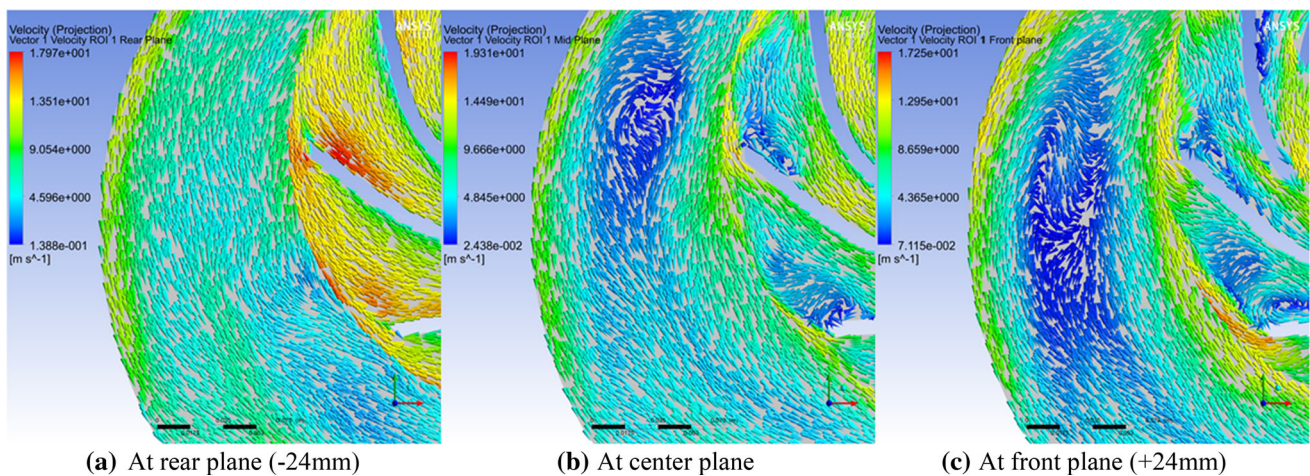


Fig. 12 Velocity vectors—transient results at the ROI 1 for existing pump

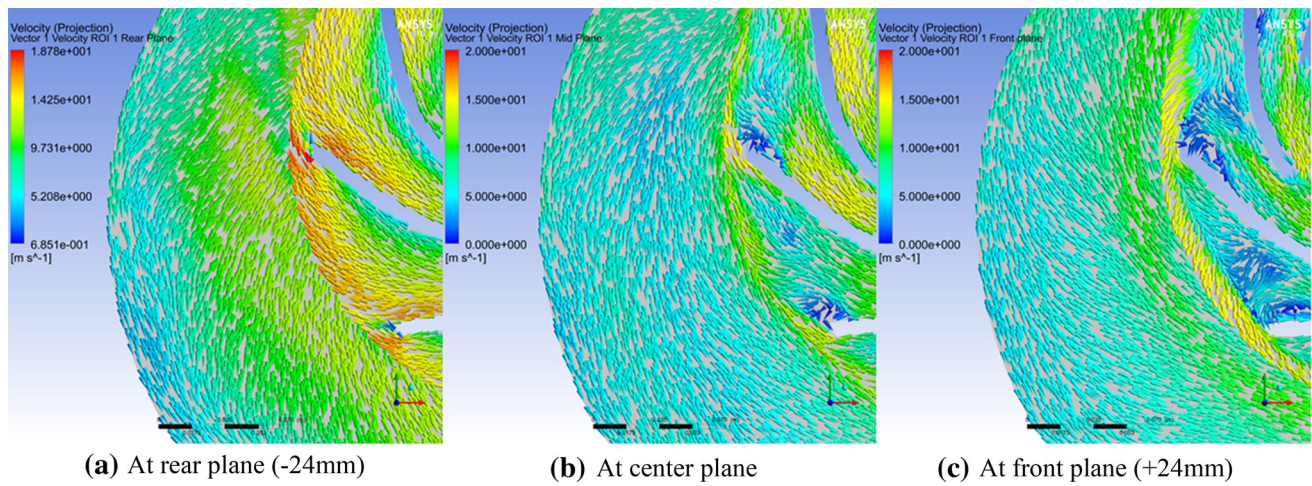


Fig. 13 Velocity vectors—transient results at the ROI 1 for modified pump (8% reduction in area)

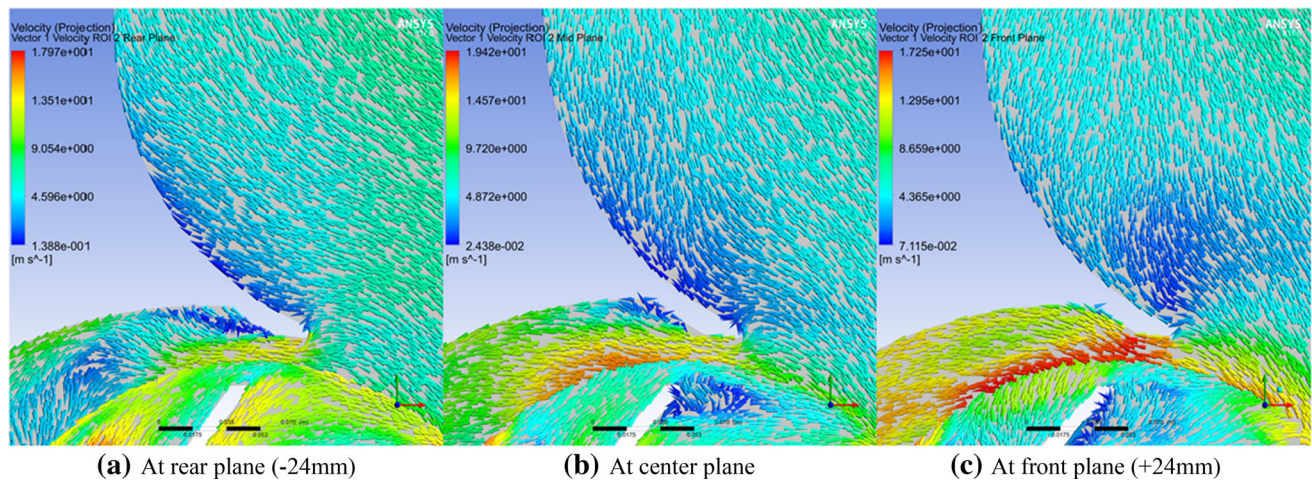


Fig. 14 Transient results at the ROI 2 for existing pump

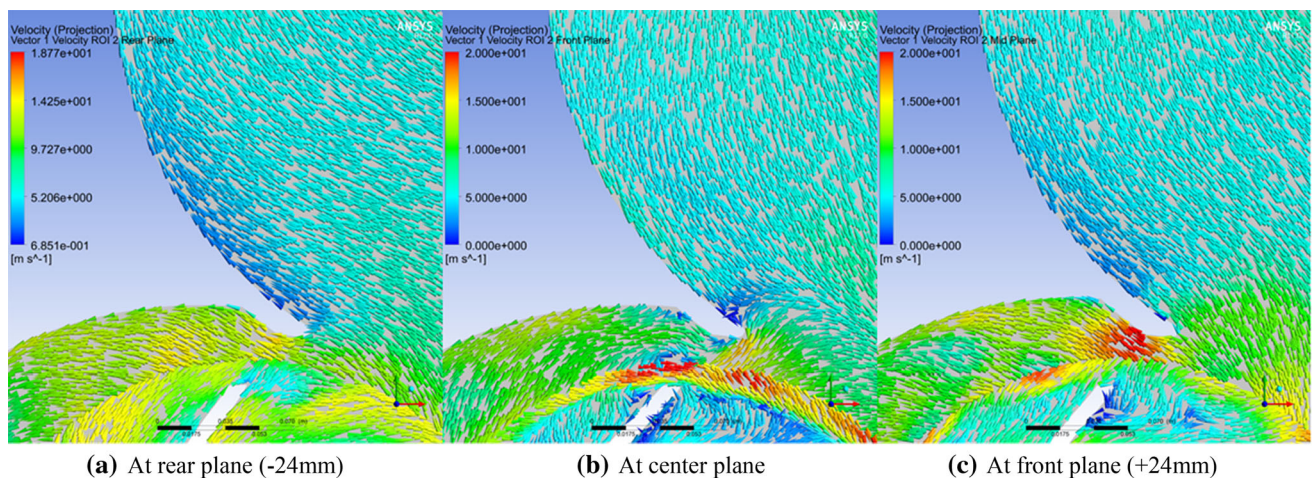


Fig. 15 Transient results at the ROI 2 for modified pump (8% reduction in area)

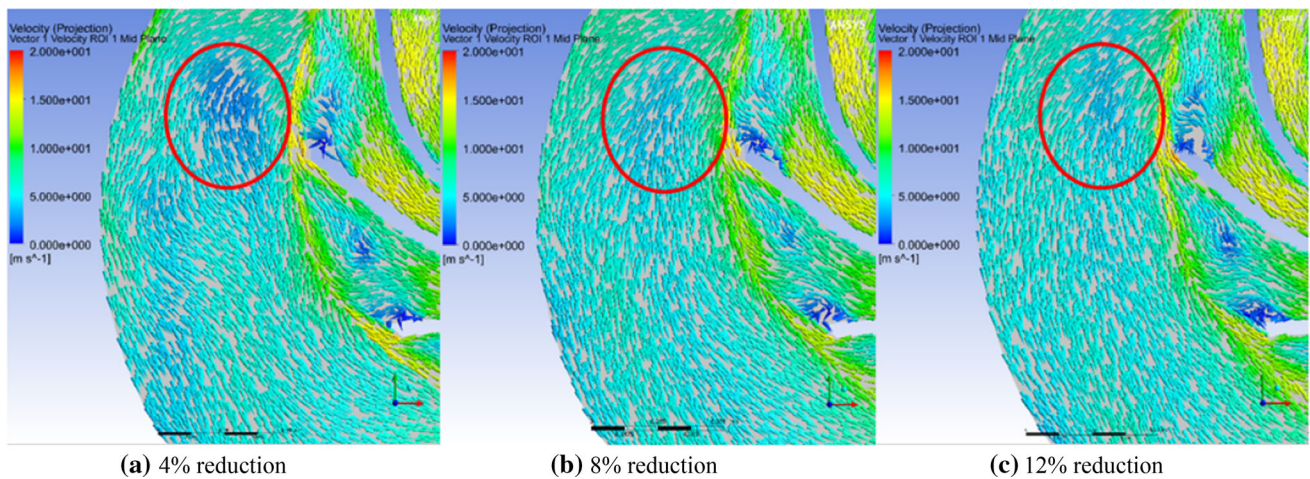


Fig. 16 Transient results at the ROI 1 for modified pump

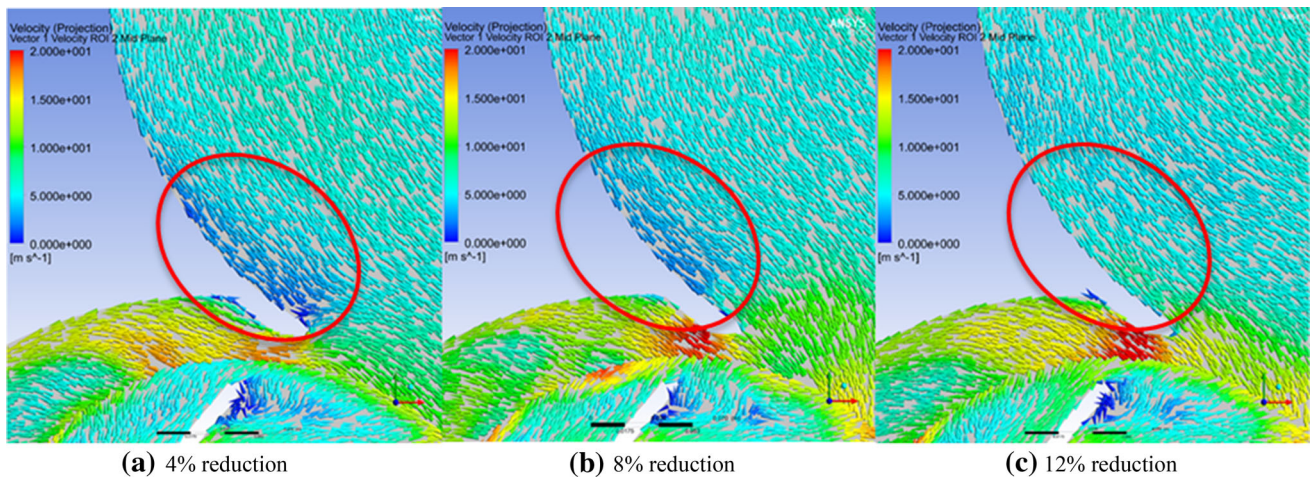


Fig. 17 Transient results at the ROI 2 for modified pump

velocity when compared to 4%. However, the model with 12% reduced area also shows some improvement over the 8% model in the regions of interest (most significant in region of interest 2). But the variables show that the hydraulic efficiency of the 12% model is lower than 8% model, due to the higher power consumed and the lower total head. This could be explained by considering that if the volume of the volute becomes too less, the backpressure increases causing disturbances of the flow in the impeller region and further increasing the effort required to push water out of the impeller region.

Performance Curves

Performance curves (CFD and experimental) are discussed for existing pump and modified pump whose area of casing was reduced by 8% at which it gives highest efficiency. The data for the curves are interpolated using cubic spline

interpolation [20]. Figure 18 shows the variation of total head with mass flow rate for both CFD (steady and transient of modified pump) and experimental (existing and modified pump) results. Comparing the two experimental curves, it is observed that the modified pump shows a higher head at and around the design flow rate of 111.11 kg/s. The transient results closely follow the curve of the modified pump. However, the steady curve is significantly different to the experimental curve. This shows the limited applicability of steady analysis to centrifugal pump problems beyond the design point. This is largely due to the increased impact of unsteady inertia effects that comes into play when moving away from the design point. At design point, the results of steady and transient are fairly close (further explained with Fig. 20). Similar results were also observed by Voorde et al. [19] in their studies.

Figure 19 shows the variation of efficiency with mass flow rate. As the mass flow rate increases, the efficiency

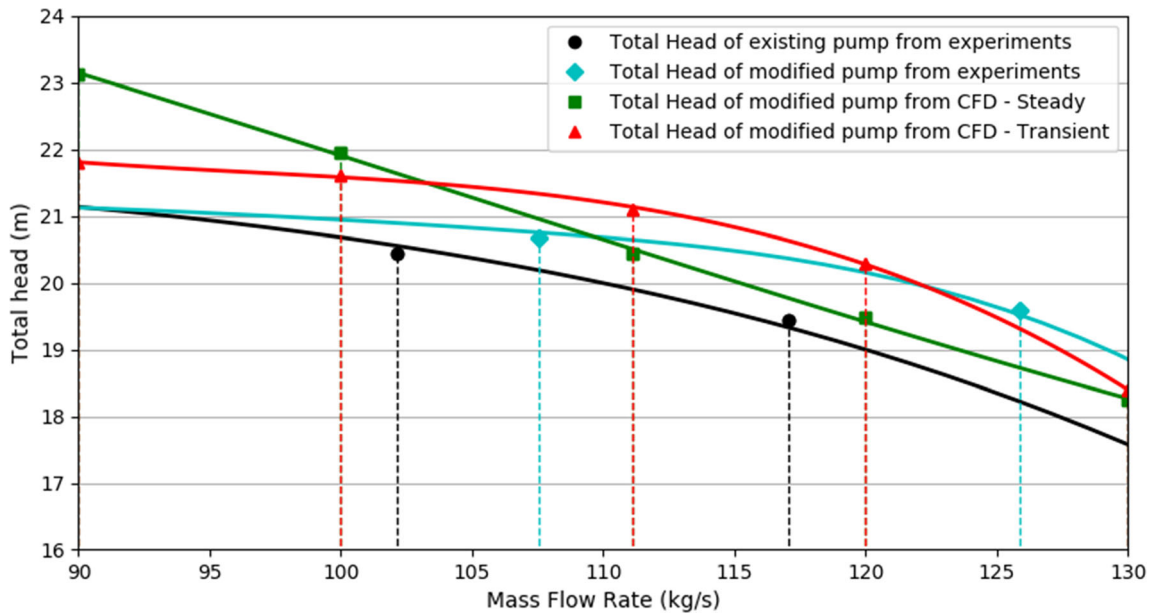


Fig. 18 Variation of total head with mass flow rate

risers to a maximum and then drops. Overall efficiency is plotted for experimental values, and hydraulic efficiency is plotted for simulation values. No mechanical or electrical efficiency was assumed to convert hydraulic efficiency of the simulation to overall efficiency. This is because the only efficiency of interest here is the relative efficiency and its improvement from existing pump to modified pump.

The experimental curve for the modified pump shows a higher efficiency at and around the design point when compared to the experimental curve for the existing pump. The peak in efficiency in experimental curve is 66.38% for

existing pump at 116.2 kg/s and 70.115% at 120 kg/s for the modified pump, a 5.63% improvement. The maximum efficiency in the transient CFD simulation is attained at a mass flow rate of 119.1 kg/s, as opposed to the design flow rate of the existing pump which is at 111.11 kg/s. At best efficiency point in CFD analysis, the efficiency increased by about 5.65% compared to the existing, from 72.81 to 76.925%. Both simulation and experimental results show similar improvement in efficiency and similar shift in BEP toward a higher mass flow rate.

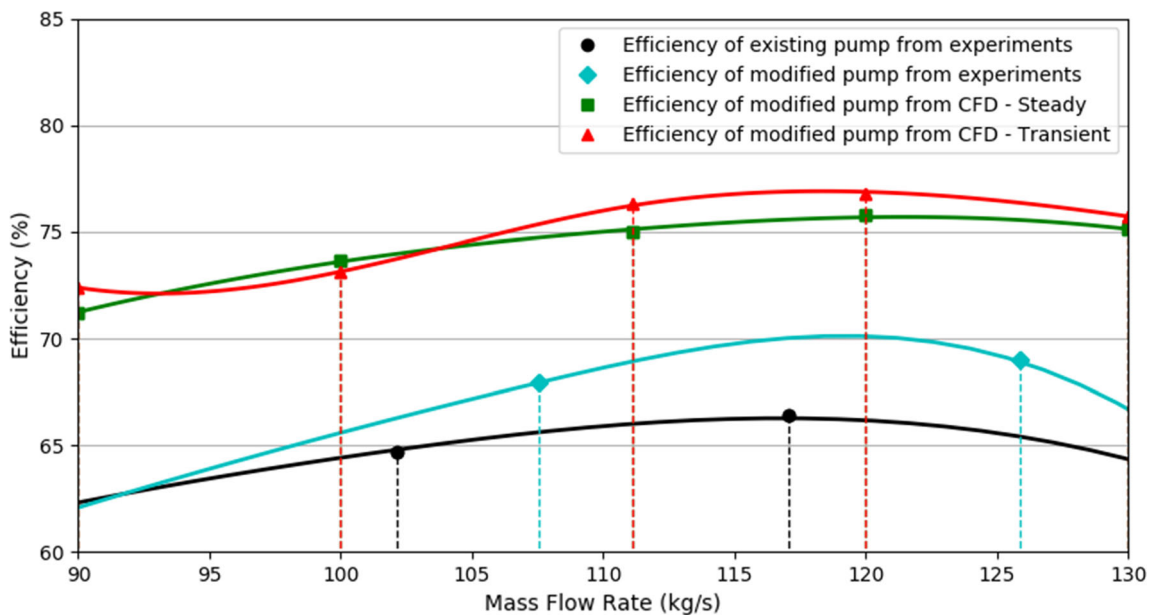


Fig. 19 Variation of efficiency with mass flow rate

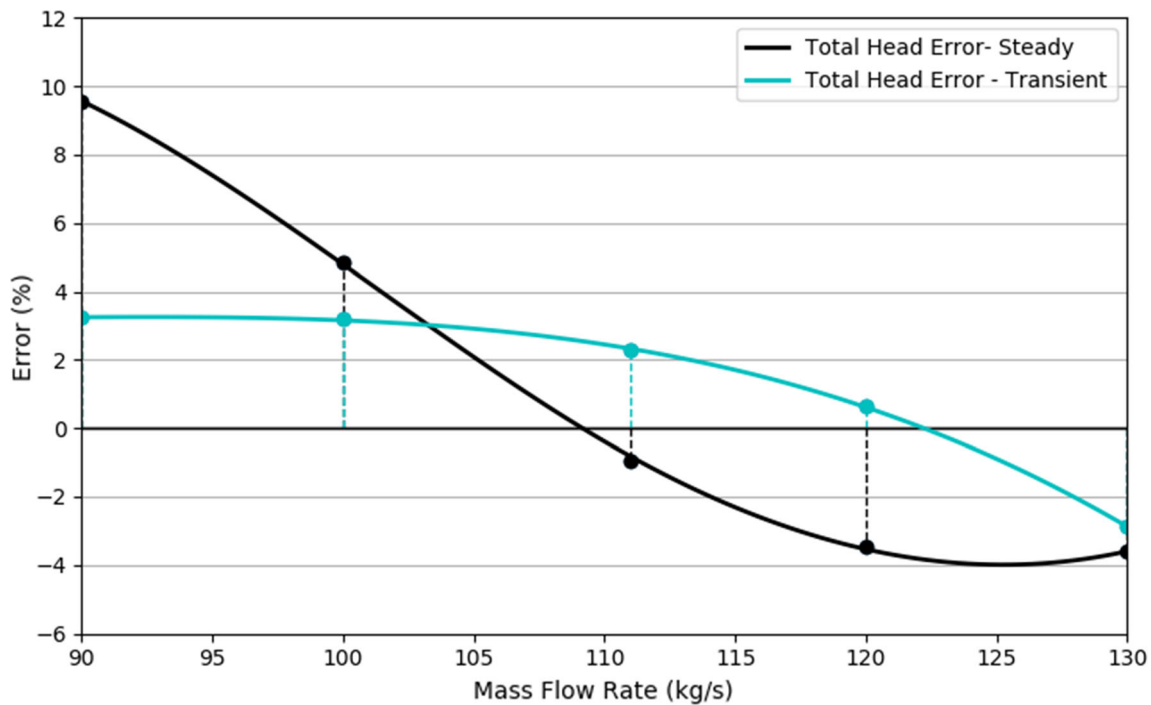


Fig. 20 Variation of error (%) in total head (CFD results) with mass flow rate (kg/s)

Figure 20 shows the variation of error in the values of total head between experiments and CFD simulations. The steady analysis gave results with a greater margin of error than transient analysis. The error for both of them is higher at off design points than at design points. The maximum error for steady-state results was 9.55%, and for transient results, it was 3.24% at 90 kg/s. The error varies wildly in steady analysis, while in transient, it hovers around $\pm 3\%$, except close to the new BEP of 120 kg/s, where it reduces to a minimum of 0.64%. As discussed in “Steady State Versus Transient Results” section, the backflow from the casing interacts with the fluid in the impeller in a transient manner due to the inertia of the fluid. Due to this, the approximation performed in steady analysis has greater error than transient analysis.

Conclusion

In this study, the effect of varying the area of volute at two locations has been studied. The changes were made to reduce losses in the pump. The new design was fabricated, and through experiments, the improvement was validated. From this study, the following conclusions can be drawn:

- The details of flow pattern within the pump are of crucial importance that affects the overall performance of the pump. The existing pump showed regions of recirculation and regions with minor losses. Modifying the design in these areas led to a significant

improvement in performance due to reduced recirculation and minor losses. The efficiency obtained through simulations shows an improvement by 4.85% at design flow rate.

- Changing the area also affects the best efficiency point. The BEP was shifted toward a higher mass flow rate of 120 kg/s. The efficiency was found to be 76.92% at BEP which is higher as compared to efficiency of existing pump (72.81%). There is 5.65% increase in efficiency for modified pump over the design point efficiency of existing pump as obtained from simulation.
- Experimental analysis validated the CFD results and showed an improvement in overall efficiency of about 4.62% from 65.96 to 69.01% at design flow rate. The percent increase in the best efficiency for the new casing is 5.63% from 66.38% to 70.115%.
- The error in the total head values of the modified pump acquired by transient simulation compared to experimental results is close to $\pm 3\%$, except near the new BEP of 120 kg/s, where it reduces to a minimum of 0.64%. The error in total head values obtained by steady analysis reaches a maximum of 9% at low mass flow rate (90 kg/s) and varies over the entire range. The transient results are more reliable and give a more realistic internal flow pattern compared to steady flow analysis.

Acknowledgements The authors wish to thank the management and employees of Process Pumps (I) Pvt Ltd for providing us the opportunity to work on this problem and for permission to publish this paper.

References

1. K. Patel, M. Satanee, New development of high head Francis turbine at jyoti ltd. for small hydro power plant, in *Proceedings of Himalayan Small Hydropower Summit*. Dehradun, India, paper, 13 (2006)
2. H. Keck, M. Sick, Thirty years of numerical flow simulation in hydraulic turbomachines. *Acta Mech.* **201**(1–4), 211–229 (2008)
3. C. Hornsby, CFD—driving pump design forward. *World Pumps* **431**, 18–22 (2002)
4. S. Yedidiah, A study in the use of CFD in the design of centrifugal pumps. *Eng. Appl. Comput. Fluid Mech.* **2**(3), 331–343 (2008)
5. D. Croba, J.L. Kueny, Numerical calculation of 2D, unsteady flow in centrifugal pumps: impeller and volute interaction. *Int. J. Numer. Methods Fluids* **22**(6), 467–481 (1996)
6. J.D. White, A.G.L. Holloway, A.G. Gerber, Predicting turbine performance of high specific speed pumps using CFD, in *ASME 2005 Fluids Engineering Division Summer Meeting 2005*, Jan (2005), pp. 125–131
7. J.H. Kim, H.C. Lee, J.H. Kim, S. Kim, J.Y. Yoon, Y.S. Choi, Design techniques to improve the performance of a centrifugal pump using CFD. *J. Mech. Sci. Technol.* **29**(1), 215–225 (2015)
8. S. Yang, F. Kong, B. Chen, Research on pump volute design method using CFD. *Int. J. Rotat. Mach.* **2**, 11 (2011)
9. E.C. Bacharoudis, A.E. Filios, M.D. Mentzos, D.P. Margaris, Parametric study of a centrifugal pump impeller by varying the outlet blade angle. *Open Mech. Eng. J.* **2**(1), 75–83 (2008). <https://benthamopen.com/ABSTRACT/TOMEJ-2-75>
10. L. Tan, B. Zhu, S. Cao, H. Bing, Y. Wang, Influence of blade wrap angle on centrifugal pump performance by numerical and experimental study. *Chin. J. Mech. Eng.* **27**(1), 171–177 (2014)
11. A.F. Ayad, H.M. Abdalla, A.A.E.A. Aly, Effect of semi-open impeller side clearance on the centrifugal pump performance using CFD. *Aerosp. Sci. Technol.* **47**, 247–255 (2015)
12. R. Spence, J. Amaral-Teixeira, A CFD parametric study of geometrical variations on the pressure pulsations and performance characteristics of a centrifugal pump. *Comput. Fluids* **38**(6), 1243–1257 (2009)
13. M.H. Shojaeefard, M. Tahani, M.B. Ehghaghi, M.A. Fallahian, M. Beglari, Numerical study of the effects of some geometric characteristics of a centrifugal pump impeller that pumps a viscous fluid. *Comput. Fluids* **60**, 61–70 (2012)
14. J. Li, Y. Zeng, X. Liu, H. Wang, Optimum design on impeller blade of mixed-flow pump based on CFD. *Procedia Eng.* **31**, 187–195 (2012)
15. B. Zhao, D. Hou, H. Chen, Y. Wang, J. Qiu, Optimization design of a double-channel pump by means of orthogonal test, CFD, and experimental analysis. *Adv. Mech. Eng.* **6**, 545216 (2014)
16. H. Roclawski, D.H. Hellmann, Rotor-stator-interaction of a radial centrifugal pump stage with minimum stage diameter, in *Proceedings of the 4th WSEAS International Conference on Fluid Mechanics and Aerodynamics* (2006), pp. 301–308
17. M. Sedlář, J. Šoukal, M. Komárek, CFD analysis of middle stage of multistage pump operating in turbine regime. *Eng. Mech.* **16**(6), 413–421 (2009)
18. S. Shah, S. Jain, V. Lakhera, CFD based flow analysis of centrifugal pump. in *Proceedings of International Conference on Fluid Mechanics and Fluid Power*, Chennai, India (2010)
19. J.V. Voorde, E. Dick, J. Vierendeels, S. Serbruyns, Performance and prediction of centrifugal pumps with steady and unsteady CFD-methods. *WIT Trans. Eng. Sci.* **36**, 559–568 (2002)
20. S. McKinley, M. Levine, Cubic spline interpolation. *Coll. Redwoods* **45**(1), 1049–1060 (1998)

Publisher's Note Springer Nature remains neutral with regard to jurisdictional claims in published maps and institutional affiliations.